Iranian Journal of Electrical and Electronic Engineering 04 (2022) 2541
Microgrid Special Issue 2022: Operation, Control, and Applications

Iranian Journal of Electrical and Electronic Engineering

Journal Homepage: ijeee.iust.ac.ir

Research Paper

Resilience Enhancement of Active Distribution Networks Via Mobile Energy Storage Systems and Protection Coordination Consideration

H. Salarvand*, M. Doostizadeh*(C.A.) and F. Namdari*

Abstract: Owing to the portability and flexibility of mobile energy storage systems (MESSs), they seem to be a promising solution to improve the resilience of the distribution system (DS). So, this paper presents a rolling optimization mechanism for dispatching MESSs and other resources in microgrids in case of a natural disaster occurrence. The proposed mechanism aims to minimize the total system cost based on the updated information of the status of the DS and transportation network (TN). In addition, the characteristics of the protection system in DS (i.e., relays with fixed protection settings), the constraints related to the protection coordination are examined under pre- and post-event conditions. The coordinated scheduling at each time step is formulated as a two-stage stochastic mixed-integer linear program (MILP) with temporal-spatial and operation constraints. The proposed model is carried out on the Sioux Falls TN and the IEEE 33-bus test system. The results demonstrate the effectiveness of MESS mobility in enhancing DS resilience due to the coordination of mobile and stationary resources.

Keywords: Mobile energy storage system, microgrids resilience, protection coordination, rolling optimization.

Nomenclature

Sets, indices

$\mathcal{T}/\mathrm{t}$	Set/ Index of time intervals
$\mathcal{N}_T/n$	Set/ Index of nodes in TN
$\mathcal{N}_D/i$	Set/ Index of buses in DS
$\mathcal{B}_D\ /(i,j)$	Set/ Index of branches in DS
$\dot{\mathcal{B}}_D^S\ /(i,j)$	Set/ Index of damaged branches in scenario s
$\mathcal{M}/m$	Set/ Index of MGs
$\mathcal{F}\ /MESS_\omega$	Set/ Index of Set of MESS fleet
$S\ /s$	Set/ Index of scenarios
$Y_T/(\hat{n},\check{n})$	Set/ Index of edges in TN
$\dot{Y}_T^S/(\hat{n},\check{n})$	Set/ Index of damaged edges in scenario s
$\mathcal{D}\ /d$	Set/ Index of depots

Parameters

$P_{D.i}^{t.s}$, $Q_{D.i}^{t.s}$	Predicted value of active/reactive load at bus i in interval t in scenario s
$\bar{P}_{ch}^{\omega}$, $\bar{P}_{dch}^{\omega}$	Maximum charging/discharging power of MESSs
η_{ch}/η_{dch}	Charging/discharging efficiency of MESSs
ΔT	Length of time intervals
ρ_s	Probability of scenario s
$\bar{S}_{ij}$	Branch power capacity
r_{ij}, x_{ij}	Resistance and reactance of line (i, j)
φ_i	Power factor (i, j)
η_{ch}^{ω} , η_{dch}^{ω}	Charging/discharging efficiency

Variables

$E_{\omega}^{t,s}$	Energy of the MESS_ω at the end of interval t in scenario s
$P_{DG,m}^{t.s}$, $Q_{DG,m}^{t.s}$	Real/reactive power generation at bus i in interval t in scenario s

Iranian Journal of Electrical and Electronic Engineering, 2022. Paper first received 31 May 2022, revised 20 Sep 2022, and accepted 01 Oct 2022

*The authors are with the Department of Electrical Power Engineering, Engineering Faculty, Lorestan University, Khorram Abad, Iran.
E-mails: hamidsalarvand740@gmail.com, doostizadeh.m@lu.ac.ir, and namdari.f@lu.ac.ir.
Corresponding Author: M. Doostizadeh.
https://doi.org/10.22068/IJEEE.18.4.2541

$I_{ch}^{\omega,t,s} I_{dch}^{\omega,t,s}$	Binary variables, battery status of $MESS_{\omega}$ in interval *t* in scenario *s*, 1 if the status is
α_{ij}^{s}	Binary variable, the connection status of branch (*i*, *j*) in scenario *s*, 1 is connected, 0 otherwise
$\partial_{\hat{n},\check{n}}^{\omega,s}$	Binary variables, 1 if the $MESS_{\omega}$ is on arc $(\hat{n},\check{n}) \in \tilde{Y}_{S}^{\omega,s}$ in scenario *s*, otherwise set to 0
$v_i^{t.s}$	Voltage magnitude at bus *i* in interval *t* in scenario *s*
I_f	Magnitude of fault current
I_p	Pickup current
$P_{ij}^{t.s}$, $Q_{ij}^{t.s}$	Real/reactive power of branch (*i*, *j*) in scenario *s*
$E_{DG.m}^{t.s}$	Energy of equivalent dispatchable DG by the end of interval t in scenario s
$P_{r,i}^{t.s}$, $Q_{r,i}^{t.s}$	Load restoration at bus *i* in interval *t* in scenario *s*
$P_{ch,m}^{\omega,t,s}$, $P_{dch,m}^{\omega,t,s}$	Charging/discharging power of $MESS_{\omega}$ from/to MG *m* in interval *t* in scenario *s*

1 Introduction

As distribution systems remain vulnerable to natural disasters, restoring the electric service effectively in response to severe power outages is indispensable, and this requires more resilient distribution systems (DSs) [1]. When severe blackouts occur, various local resources in microgrids (MGs) and distributed energy resources can be utilized to restore critical loads in DSs. Moreover, emerging mobile energy storage systems (MESSs) can provide temporal-spatial mobility and they can be coordinated with stationary local resources to restore the DS. Therefore, efficient outage management is one of the critical requirements for resilient DSs. Resilience refers to the ability of a system to return itself, with little or no human intervention, to a safe and secure operation from any disruption or interruption [2]. The structure of a DS and the quality of its operation originate from the engineering design process. There is a significant relationship between the degree of design quality, operating rate, and increasing resilience of the DS. Therefore, network designers face many challenges in designing and developing DSs. Environmental changes, climate patterns, natural disasters such as floods and earthquakes, new technologies, and the increasing number of customers influence the network, its design, and its resilience. Resilience methods in DSs can be seen in two actions: A) Retrofitting or hardening measures: these measures are taken to boost the resilience of infrastructure, and B) Smartening or operational measures: these measures are taken to boost operational resilience.

Hardening measures might be more resilience-effective than the operational ones but are less cost-effective [3]. Operational measures take advantage of incoming information about the external shock through forecasting tools and, thus apply actions in proportion to the prevailing conditions. The smart solutions aim at enhancing the operational resilience of a power grid. Generating, storing, and controlling energy locally without relying on long DSs, which might be prone to different threats, can make the network less vulnerable and improve response time and restoration. Network resilience studies require systematically analyzing several components (vulnerability, compatibility, and restoration ability) and their interactions under adverse scenarios.

The relationship between the resilience of the power grid and the power generation, especially using the distributed generation (DG), has been studied in the literature concerning the design of resilient DSs. Specifically, optimized allocation and operation of renewable energy sources in MGs have been shown to improve the resilience of the grids [4]. So, they can be used for planning, response and restoration of the power grid [5]. Great progress has been made in utilizing stationary resources for service restoration in DSs after major blackouts [6, 7]. The resilience response framework is also presented by re-dispatching the generator, switching topology, and shedding loads [8].

After a natural disaster, multiple damages are very probable. So, repair crews play a critical role during the restoration stage. The efficient management [9] and the allocation [10] of repair crews reduce restoration time and customer disconnections and increase DS resilience. Moreover, network reconfiguration is often applied as a basic operational measure to enhance the resilience of DSs [4], [11]. Hence, fast and efficient load restoration based on network reconfiguration is a basic and key step to enhancing the resilience of DSs in extreme weather events. Various research studies have also used mobile batteries to enhance network resilience. For example, in [12], the MESS has enhanced network resilience. In [13], a two-stage scheduling procedure has been introduced for the resilient operation of MESSs in DSs. In the first stage, mobile sources are pre-positioned to support the rapid restoration of the disruptions, which in turn

assist in surviving critical loads. In the second stage, i.e., after the event, the mobile power sources will be dispatched and coordinated to enhance the restored loads. For normal operations, MESSs are also employed to achieve load shifting [14] and relieve transmission congestion [15]. A sequential framework has been suggested to pre-position mobile generators for staging locations and real-time dispatching to DSs [16]. The stochastic modeling of MESSs via a time-space network is formulated to investigate the vehicle routing and scheduling problem in [17] and [18].

The contribution of the MGs based on their resources such as DG and MESS to the resilience enhancement of the networks in areas prone to extreme weather has been demonstrated in several real cases [19]. In [20], the formation of dynamic MGs has been applied to accommodate mobile and stationary DG and energy resources after disruptions. For post-disaster restoration, [21] has proposed a resilient design, including scheduling repair crews, mobile power sources, and network reconfiguration.

Recent studies that suggest applying of MESSs still require more precise stochastic modeling in the DS, since extreme weather events can destroy the DSs and some other interdependent infrastructures [22] and [23]. At the time of a natural disaster, not only is there a possibility of damaging the DS, but to the roads along which the MESSs are connected to the DS are likely to be damaged. Besides, the presence of MESSs and DGs leads to changes in electrical parameters in the DS due to the radial structure and the protection design of the DS. Ignoring the impact of these resources at the time of network reconfiguration may disrupt the protection coordination of the DS. One of the important features of the inverter-based sources like MESSs is the ability of their converters to limit the level of short circuit current to less than 200% of the rated current and specially to prevent participation these resources to the fault current. At the time of a fault in a MG, they reduce the short circuit level in the shortest possible time and prevent the possible damages for the resources and the MG. If the MG is connected to the upstream grid, these inverter-based sources may cause the relays to malfunction by limiting the fault current to a value between 1.2 and 2 on the per-unit scale [24].

Few existing studies considered the load service restoration in an integrated DS and transportation network (TN). An integrated restoration strategy is needed to coordinate the mobile and stationary resources for service restoration with dynamically updated system damage information in coupled TN and DS. In addition, reviewing previous research on resilience enhancement and restoration of critical loads especially via stationary and mobile energy sources in DS indicates the lack of attention to protection coordination in normal and post-event conditions as well as the protection elements with the ability to adjust settings.

To address the above research gaps, this paper proposes a model to load restoration of a DS via DGs and MESSs in which the protection system operates correctly under the changes in the network topology. To do so, a two-step algorithm is proposed to coordinate the existing protection systems, increase resilience, and optimally reconfigure the DS. Since the coordination of relays and other protection devices with fixed and basic settings is not reliable to cover any islanding conditions, the first step is to check all MG disconnection modes to determine the amount of passing current and short circuit to achieve a reliable, coordinated, and error-free protection system setting under new topology. In the second step, MESSs are reconfigured and used in the optimal return routes. In this study, a semi-smart DS with adjustable protection relays is studied [25].

The rest of this paper is organized as follows: Section 2 describes the proposed model; Section 3 presents the proposed algorithm; Section 4 provides numerical studies on a case study and compares different scenarios to verify the effectiveness of the proposed method; and Section 5 concludes the paper.

2 Proposed Model

The increasing emergence of MESSs highlights their superiority over stationary resources in terms of mobility and flexibility. When a blackout happens, the MESS can be dispatched among MGs to transport power and restore the load. As soon as an event occurs, one or more MGs are disconnected, and some loads are lost, the network configuration is changed to preserve the radial nature and prevent definite propagation, and alternative lines are used. In this situation, the MESSs have to reach the desired MG and bus based on the importance of the loads. Based on the initial information of the damaged branches of the DS and TN, the MESSs are programmed and moved to the bus and the MG with a higher priority of load restoration.

The return routes of the MESSs to the depot and their movements between the MGs may be damaged

and need to be replaced with the new route(s). The MESS must cross through different routes to reach the desired bus to be able to charge or discharge. Certainly, such routes are subject to events in adverse weather conditions, and this issue should also be considered as one of the uncertainties. In addition to the damage to and repair of roads in TN, the proposed model also considers damage and repair of branches and uncertainty of load consumption in the DS. To account the uncertainties and issues related to the road maintenance scheduling in the TN, a scenario-based stochastic time-space network is proposed to model the temporal-spatial behavior of MESSs over the TN. The uncertainties in damage and repair to the roads in TN and the branches in DS are modeled via Monte-Carlo simulation and the obtained scenarios are also reduced to finite set of uncertainty scenarios. The normal distribution function with the standard deviation of 2% is used to represent the load forecast error, [26]. Also, a two-state Markov model is applied to represent the availability of roads and branches [27], while the available and unavailable hours are a function of exponential distribution function. Then, a set of scenarios s is created using the Monte Carlo simulation method. In order to reduce the computational efforts, a simultaneous backward reduction method [27] is adopted to reduce the number of scenarios a good approximation of the uncertainty of the system. The subset of scenarios and a probability measure based on this subset are determined so that is the closest to the initial probability distribution in terms of probability metrics. During the restoration process, instantaneous information about the return routes (safe, defective, or repaired) and power outages are received. Consequently, a rolling horizon optimization framework has been considered to dynamically update the system damage status and reschedule the MESS fleet. To do so, the whole time horizon $\mathcal{T}_H$ is discretized into equal time intervals by Δt and the optimization problem is formulated and solved at each time interval over the forecasted horizon $\mathcal{T}_P$, but only the results in the first interval are implemented. Then the forecasted horizon is moved forward and the calculation is repeated for the new forecasted horizon until the end of the whole time horizon $\mathcal{T}_H$, according to the updated system information and initial conditions. The final decisions are the series of the decisions in the first interval of each forecasted horizon.

The battery charging/discharging schedule and temporal-spatial constraints are also addressed in the proposed model. The MESS travel starts from the depot, and a matrix with three features (The shortest path, Distance and Travel time) are calculated. The damage to and repair of the roads in TN influence the elements of this matrix and lead to the reconstruction of time-space arcs in the time-space network. So, the temporal-spatial behavior of MESS fleet is modeled through a time-space network.

While the protection settings change due to passing currents and short circuits metamorphosis, reliable protection settings are added to the rolling optimization problem using the constraints related to the operation and coordination of the protection system in DS. Constraints related to MESSs, DS, and protection systems are presented in the following.

2.1 Constraints of MESS

TN information is considered with two parts: node and edge. The TN is modeled as a weighted graph, $G_T = (\mathcal{N}_T. Y_T. \mathcal{W}_T)$. An MESS $\omega \in \mathcal{F}$ is initially located at a depot $\in \mathcal{D}$, where it starts and travels among MGs to provide energy to the DS, and finally it goes back to a depot. For scenario *s*, the shortest path matrix is used to describe the shortest paths for all pairs of MGs or depots. Accordingly, shortest path element g_{ij}^s denotes the set of nodes $\mathcal{N}_{ij}^s$ and edges Y_{ij}^s with edge distances $\mathcal{W}_{ij}^s$ in the route, which is calculated by Dijkstra's algorithm [28].

$$g_{i\,j}^s = \left(\mathcal{N}_{ij}^s \text{ و } Y_{ij}^s \text{ و } \mathcal{W}_{ij}^s\right), \forall i,j \in \mathcal{M} \cup \mathcal{D}, s \quad (1)$$

The sum of the edge distances along the shortest path is used to calculate the distance element $\wp_{ij}^s$ as in (2).

$$\wp_{ij}^s = \sum_{n \epsilon \mathcal{W}_{ij}^s} l\,, \forall s \quad (2)$$

Therefore, the travel time element in the number of intervals considering average speed of MESSs (V_{avg}^{ω}) can be calculated as follows:

$$t_{ij}^s = \left\lceil \wp_{ij}^s / V_{avg}^{\omega} / \Delta t \right\rceil, \forall MESS\ \omega \in \mathcal{F}, i,j \in \mathcal{M} \cup \mathcal{D}, s \quad (3)$$

where $\lceil \quad \rceil$ is the ceiling function.

If the MESS ω starts at the depot, g_{ij}^s, $\wp_{ij}^s$ and t_{ij}^s are obtained. Then temporal-spatial behavior of the MESS will be modeled through a time-space network.

For example, in Fig. 1, suppose in one scenario the road 14-23 is damaged at the first hour and will

be repaired at hour 3. The shortest path, the distance and travel time from depot to MG #4 changes due to the road damage. The original routes and updated routes are respectively denoted as the black and green dash lines in Fig 1.

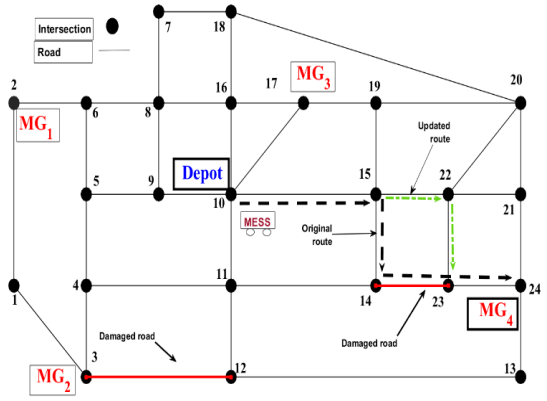

Fig. 1 A TN connected to MGs and a depot.

A. Temporal-spatial Constraints

The temporal-spatial behavior of MESSs over the TN (G_T) is converted into the multi-layer time-space network. The scheduling of MESS is defined as a series of trips by time-space arcs starting from a source node ($\hat{n}$) to the time-space nodes of the MG, and finally returning to a sink node ($\check{n}$). The formulation is based on arc wise binary variables $\partial_{\hat{n}.\check{n}}^{\omega.s}$, which are set to 1 if the MESS is on an arc $(\hat{n}.\check{n}) \in \tilde{Y}_S^{\omega.s}$ in scenario s, otherwise set to 0 [29]. Moving arc $\tilde{Y}_S^{\omega.s}$ connects two MG time-space nodes and represents a movement in spatial and time dimensions in scenario s. MESS can only be on exact one arc in any time interval. The MESS's states can be described by constraint (4).

$$\sum_{(\hat{n},\check{n})\in\tilde{Y}_S^{\omega.s}} \partial_{\hat{n}.\check{n}}^{\omega.s} = 1\ , \forall m, \omega, t, s \tag{4}$$

The time-space network flow conservation can be formulated via constraints (5) and (6).

$$\sum_{(\hat{n},\check{n})\in\acute{\varepsilon}_{s,n}^{\omega.s}} \partial_{\hat{n}.\check{n}}^{\omega.s} = \sum_{(\hat{n},\check{n})\in\grave{\varepsilon}_{s,n}^{\omega.s}} \partial_{\hat{n}.\check{n}}^{\omega.s}\ \forall n\epsilon\widetilde{\mathcal{N}}_S^{\omega.s}, \omega, s \tag{5}$$

$$\sum_{(\hat{n},\check{n})\in\grave{\varepsilon}_{s,n}^{\omega.s}} \partial_{\hat{n}.\check{n}}^{\omega.s} = \partial_{init}^{\omega.s}\ \forall n\epsilon\widetilde{\mathcal{N}}_S^{\omega.s}, \omega, s \tag{6}$$

For each time-space node $n\epsilon\widetilde{\mathcal{N}}_S^{\omega.s}$ in scenario s, the time-space arcs connecting the n can be categorized into two groups of in-flows $\grave{\varepsilon}_{s,n}^{\omega.s}$ and out-flows $\acute{\varepsilon}_{s,n}^{\omega.s}$ representing the arcs entering or leaving the n, respectively. For source nodes $n\epsilon\widetilde{\mathcal{N}}_S^{\omega.s}$, there are out-flows with the initial location of MESSs. Each time-space node n should fulfill the network flow conservation. In other words, the $MESS\ \omega$ end s trips at time-space node n serving as the starting point of the later trip. The $\partial_{init}^{\omega.s}$ indicates the MESS's initial location.

B. Operational Constraints

When staying on a holding arc, a MESS can exchange power with DS by charging or discharging. Following constraints state the relation between charging/discharging power and temporal-spatial behaviors. Holding arc $\bar{Y}_S^{\omega.s}$ connects two time-space nodes for the same MGs in a time interval in scenario s.

$$0 \le P_{ch,m}^{\omega,t,s} \le \partial_{\hat{n},\check{n}}^{\omega,s}\bar{P}_{ch}^{\omega}, \forall(\hat{n},\check{n}) \in \bar{Y}_{S,m}^{\omega,t,s}, \omega, m, t, s \tag{7}$$

$$0 \le P_{dch,m}^{\omega,t,s} \le \partial_{\hat{n},\check{n}}^{\omega,s}\bar{P}_{dch}^{\omega}, \forall(\hat{n},\check{n}) \in \bar{Y}_{S,m}^{\omega.t.s}, \omega, m, t, s \tag{8}$$

Equations (9) and (10) express the charging/discharging power associated with battery status, which is constrained by temporal-spatial behaviors in (11).

$$0 \le \sum_{m\in\mathcal{M}} P_{ch.m}^{\omega.t.s} \le I_{ch}^{\omega.t.s}\bar{P}_{ch}^{\omega}, \forall\omega, t, s \tag{9}$$

$$0 \le \sum_{m\in\mathcal{M}} P_{dch.m}^{\omega.t.s} \le I_{dch}^{\omega.t.s}\bar{P}_{dch}^{\omega}, \forall\omega, t, s \tag{10}$$

$$I_{ch}^{\omega.t.s} + I_{dch}^{\omega.t.s} \le \sum_{(\hat{n},\check{n})\in\bar{Y}_{S.m}^{\omega.t.s}} \partial_{\hat{n}.\check{n}}^{\omega.s}, \forall m, \omega, t, s \tag{11}$$

The following equations limit the state of charge (SOC) of each MESS.

$$E_{\omega}^{t.s} = E_{\omega}^{t-1.s} + \eta_{ch}P_{dch.m}^{\omega.t.s\ \omega} - \frac{1}{\eta_{dch}}P_{dch.m}^{\omega.t.s}\forall\omega, t, s \tag{12}$$

$$\underline{SOC}^{\omega} \le E_{\omega}^{t.s} \le \overline{SOC}^{\omega}\forall\omega, t, s \tag{13}$$

2.2 Constraints of DS and MGs

A DS is modeled as a graph, $G_D = (\mathcal{N}_D.\mathcal{B}_D)$ [7]. A linearized distribution power flow model [30] is employed for power flow analysis. A linearized three-phase power flow can be included to further extend this model to unbalanced three-phase conditions [31]. To keep the grid radial in any reconfiguration, the following constraint should be addressed:

$$\sum_{(i.j)\in\mathcal{B}_D} \alpha_{ij}^{s} = |\mathcal{N}_D| - |\mathcal{M}|, \forall s \tag{14}$$

where $|\mathcal{N}_D|, |\mathcal{M}|$ represent the cardinality of the sets. The following equation represents the damaged branch status.

$$\alpha_{ij}^{s} = 0, \forall (i,j) \in \dot{\mathcal{B}}_D^s, s \quad (15)$$

The following constraints describe the active and reactive power balance at bus i.

$$P_{G,i}^{t.s} - P_{r,i}^{t.s} = \sum_{(i.j)\in\mathcal{B}_D} P_{ij}^{t.s} - \sum_{(k,i)\in\mathcal{B}_D} P_{ki}^{t.s}, \forall i,t,s \quad (16)$$

$$Q_{G,i}^{t.s} - Q_{r,i}^{t.s} = \sum_{(i.j)\in\mathcal{B}_D} Q_{ij}^{t.s} - \sum_{(k,i)\in\mathcal{B}_D} Q_{ki}^{t.s}, \forall i,t,s \quad (17)$$

The inequality constraints (18) and (19) are used to keep the voltage magnitudes within the proper range and set the voltage of MGs' buses to v_0.

$$v_{imin} \le v_i^{t.s} \le v_{imax}, \forall i \in \mathcal{N}_D \backslash G_D(\mathcal{M}), t, s \quad (18)$$

$$v_i^{t.s} = v_0, \forall i \in \mathcal{N}_D \quad (19)$$

The following inequalities depict the power capacity constraints of each dispatchable DG.

$$0 \le P_{DG,m}^{t.s} \le \bar{P}_{DG,m}, \forall m,t,s \quad (20)$$

$$-\bar{Q}_{DG,m} \le Q_{DG,m}^{t.s} \le \bar{Q}_{DG,m}, \forall m,t,s \quad (21)$$

Equation (22) tracks the energy of each MG.

$$E_{DG,m}^{t+1.s} = E_{DG,m}^{t.s} - P_{DG,m}^{t+1.s}\Delta t, \forall m, t \in \mathcal{T}_P \quad (22)$$

The energy level within each MG is limited by (23).

$$\underline{E}_{DG,m} \le E_{DG,m}^{t.s} \le \bar{E}_{DG,m}, \forall m,t,s \quad (23)$$

2.3 Constraints of DS protection system

A. Relay performance constraints

The operation of the relay in short circuit condition depends on the fault current to the pickup current ratio. According to the standards IEC, ANSI/IEEE, the operation characteristic or time-current characteristic (TCC) of the relay can be adjusted according to the following equation:

$$t_{op} = \frac{TMS \times \beta}{\left(\frac{I_F}{I_P}\right)^{\alpha} - 1} + L \quad (24)$$

where β, α, L are constant coefficients; I_F is the fault current magnitude; I_P is the pickup current value; and TMS is the time multiplier setting. I_P and TMS should be within a specific range for over current relays, as presented in the following equations [32].

$$TMS_{min} \le TMS \le TMS_{max} \quad (25)$$

$$I_{Pmin} \le I_P \le I_{Pmax} \quad (26)$$

For phase relays, the pick-up current above the nominal current is determined via the overload factor (OLF) to provide a margin for the over load conditions. It can be formulated as follows:

$$I_P = OLF \times I_{nom} \quad (27)$$

where I_{nom} refers to the nominal current at the relay location.

B. Constraints of coordination between relays

The coordination between the relays and the re-closer is such that the relay, at the time of a re-closer failure, waits at least as long as the total power outage time. It will cut off the fault current if the re-closer is not working properly. The coordination time interval (CTI) as the operating time difference between primary and backup relays represents this coordination as in (28).

$$t_{ij}^{b} - t_i^{p} \ge CTI \quad (28)$$

Where t_i^p is the operating time of the primary relay, and t_{ij}^b is the operating time of the backup relay. If the time difference between the two relays is less than 0.3 and the time interval is not observed, more or less both relays operate together, therefore, $t_{ij\,new}$ is calculated with a minimum time difference of 0.3 from t_{ij}:

$$\text{If } CTI \le 0.3, \text{ then } t_{ij\,new} = t_{ij} + 0.3 \quad (29)$$

To obtain the most TMS protection equipment, a normal relay, with IEC 60255 standard, and α = 0.02, β = 0.14, and TMS = 0.05 (initial value), is considered and different network conditions are studied. Accordingly, by changing (29) and by the required distance, the new TMS of upstream relay is calculated.

$$TMS_{new} = \frac{\left(\frac{I_F}{I_P}\right)^{\alpha} - 1}{\beta} * t_{op1\,new} \quad (30)$$

2.4 Objective functions

The first objective function is formulated as follows to minimize the operating time of the relays:

$$\boldsymbol{OF1} = min(\Sigma_{m=1}^{1}\Sigma_{f=1}^{f}\,(t_i^p + \Sigma_{j=1}^{j} t_{ij}^b)) \quad (31)$$

where *f* indicates the position of the fault; *i* refers to the primary relays (the total number of relays is *N*); *j* denotes backup relays; *t* denotes the relay's operating time, and *m* indicates the operating mode of the MG (1 denotes the network connection mode and 2 indicates the islanding mode).

The second objective function is formulated as follows to minimize the total cost.

$$\boldsymbol{OF2}$$
$$= min\ (\sum_{t=1}^{24} \rho_s \sum_{s\in S} \left[\left[\sum_{i\in \mathcal{N}} W_i (P_{D.i}^{t.s} - P_{r.i}^{t.s}) + \sum_{m\in \mathcal{M}} C_{gen.m} P_{DG.m}^{t.s} + \sum_{\omega\in\Omega} C_{bat.\omega} \sum_{m\in\mathcal{M}} (P_{ch.n}^{\omega.t.s} + P_{dch.m}^{\omega.t.s}) \right] \Delta t + \sum_{\omega\in\Omega} C_{tran.\omega} \sum_{(\hat{n}.\check{n})\in Y_S^{\omega.s}} \partial_{\hat{n}\check{n}}^{\omega.s} \right]). t \in \mathcal{T}_P \quad (32)$$

Where the term $\sum_{t\in\mathcal{T}_P}\sum_{s\in S}\sum_{i\in\mathcal{N}} W_i(P_{D.i}^{t.s} - P_{r.i}^{t.s})\Delta T$ is the customer interruption cost; the term $\sum_{t\in\mathcal{T}_P}\sum_{s\in S}\sum_{m\in\mathcal{M}} C_{gen.m}P_{DG.m}^{t.s}\Delta T$ shows the MG generation cost; the third term $\sum_{t\in\mathcal{T}_P}\sum_{s\in S}\sum_{\omega\in\Omega} C_{bat.m}\sum_{m\in\mathcal{M}}(P_{ch.n}^{\omega.t.s} + P_{dch.m}^{\omega.t.s})\,\Delta T$ calculates the MESS battery maintenance cost; and the last term $\sum_{s\in S}\sum_{\omega\in\Omega} C_{tran.\omega}\sum_{(\hat{n}.\check{n})\in Y_S^{\omega.s}} \partial_{\hat{n}\check{n}}^{\omega.s}$ denotes the transportation cost.

2.5 Resilience measure

The proposed model aims to maximum critical loads restoration and resilience improvement by planning the direction of mobility MESS and coordinating with DGs in MGs. Whereas attention to the required infrastructure such as accessible roads is also was considered in planning and optimization. The proposed model considers the indicators that resilience measure as a static quantity and a function of time. The Distribution Risk Index (DRI) is presented in this paper to evaluate the resilience of DS. This index consists of two parts, and is calculated via (33). The necessity of using this criterion is to consider network resilience indicators for load supply and the resilience index of scattered production sources together to obtain the resilience of the entire network.

$$DRI = DRI_{load} - GRI_{DG} \quad (33)$$

DRI_{load} represents the resilience of the network in terms of providing load, which expresses the amount of load lost in DS when unexpected events occur. The lower the value of this index, the greater the resilience of the network. The availability of these resources is particularly important when events occur. In many cases due to the unavailability of DG, it is not possible to feed the load.

Generation Resiliency Index (GRI) stands for the amount of production DG available. The larger the value of this index, the greater the resilience of the network. The higher the GRI and the lower the DRI, the better the resilience of the entire network. Therefore, the lower the value of DRI in (33), the greater the resilience of the network. The presence of MESS in islanded MGs with lack of DG can lead to GRI greater and the presence of MESS in MG with DGs will increase the GRI.

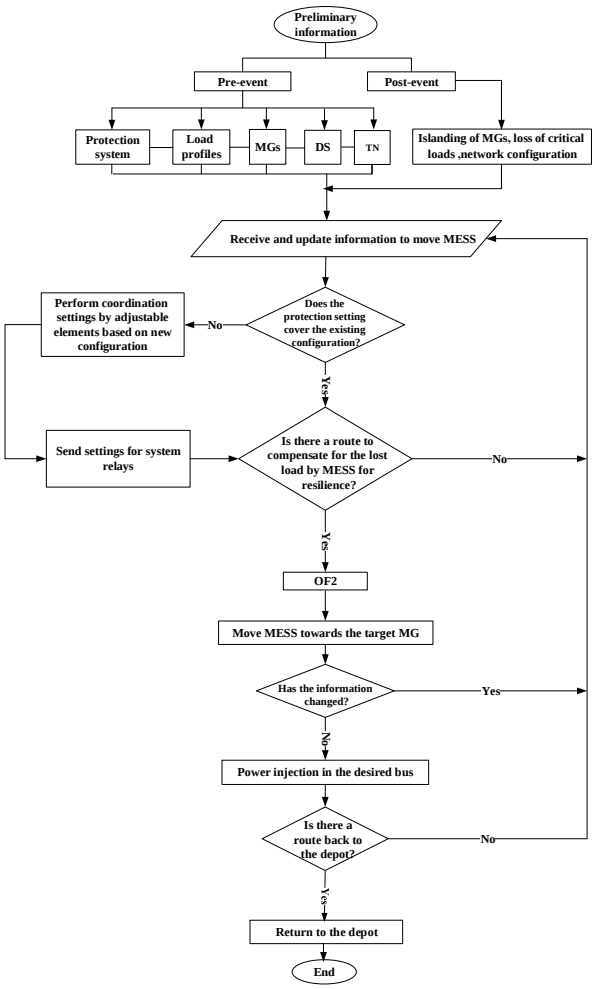

Fig. 2 The flowchart of proposed method for smart DS.

3 Proposed solution algorithm

In previous literature, increase of resilience especially using MESSs, protection constraints have been less discussed and DS were considered to be smart and capable of adapting protection settings in any configuration for system relays. In real DS, such conditions do not exist due to the lack of advanced telecommunication platforms and presence of large numbers of branches. Therefore, the two mentioned cases are addressed. In first model, the DS is assumed to be sufficiently smart. So, relay settings are coordinated, and necessary adaptions are done in accordance with the new configuration (as shown in Fig.2).

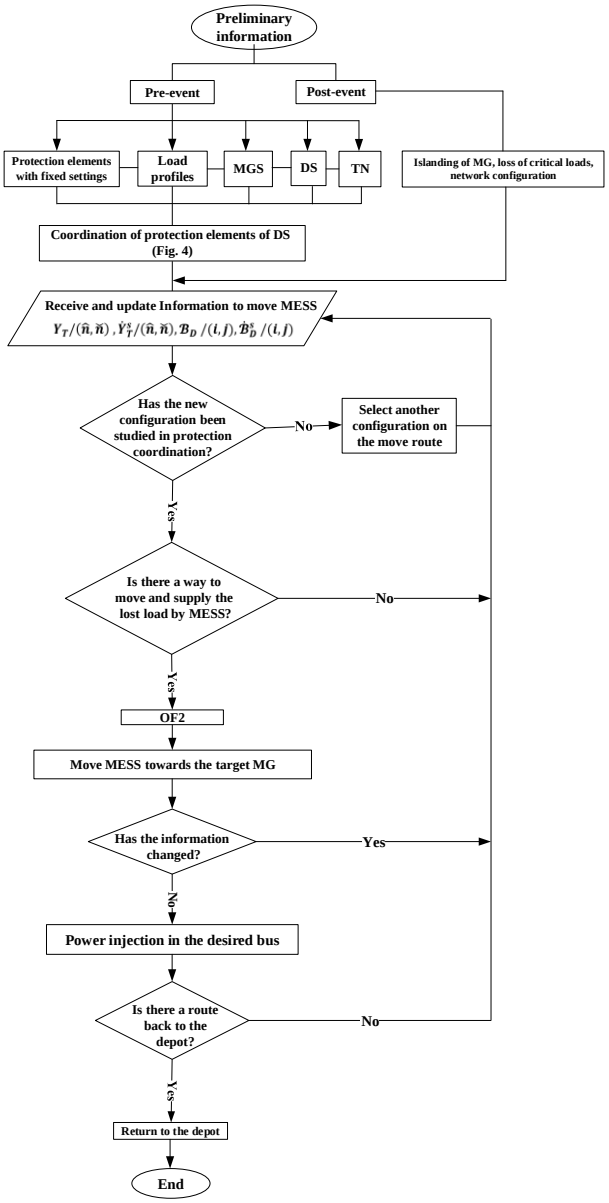

Fig. 3 The flowchart of proposed method for current DS.

In the second model, the DS is considered with protection elements and without the possibility of sending the relays settings for the new structure(s). According to Fig. 3, basic information for normal condition of DS, protection elements, and the traffic routes between the MGs are available. As soon as an event occurs, and one or more MGs are disconnected. So, the basic information changes, and a number of critical loads are lost. Then, MESSs start moving from the depot to the desired MG and buses based on the updated information, and the weight and prioritization of loads in the lowest cost manner. For better presentation, the protection coordination is shown in Fig. 4. After the event and the islanding of the MG(s), the load reduction and network reconfiguration will lead to changes in the passing current and short circuit. The initial protection settings are fixed and may be uncoordinated in such situations (even when connecting MESSs to the network). According to Fig. 4, changes in short circuit level and branch current are calculated for all the islanding modes of MGs. Then, the operating time of the relays is set by determining the appropriate TMS, and the necessary and reliable coordination is determined based on the objective function ((1)). If protection coordination is not considered for a configuration in post-event, another configuration and route with protection coordination will be replaced.

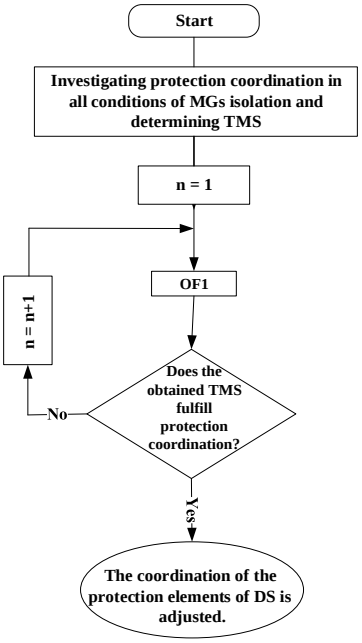

Fig. 4 Protection coordination flowchart.

After checking the protection coordination, MESSs receive the latest information on DS and TN traffic (exiting the depot, moving between nodes, and returning to the depot). In fact, a rolling optimization is considered for scheduling and next actions. As it is evident from Fig. 3, after determining the direction of travel, the MESSs move to restore critical loads based on the second objective function and they reach the desired buses or MGs. Finally, returning to the depot is done by receiving the latest information on TN and choosing the optimal route.

4 Numerical studies

In order to show the validity and effectiveness of the proposed model, several studies were carried out on an integrated system including the modified IEEE 33-bus distribution network [33] with protection elements and the Sioux Falls TN [34]. The TN and DS test systems are shown in Figures 5 and 6,

respectively. The protection system of DS was considered with a normal inverse time overcurrent relay device as the primary relay and 8 re-closer devices as secondary relays. As MGs are the interface between TN and DS, other buses and branches of DS cannot directly be linked to the TN. That is why only the MGs locations are explicitly indicated in Fig. 5.

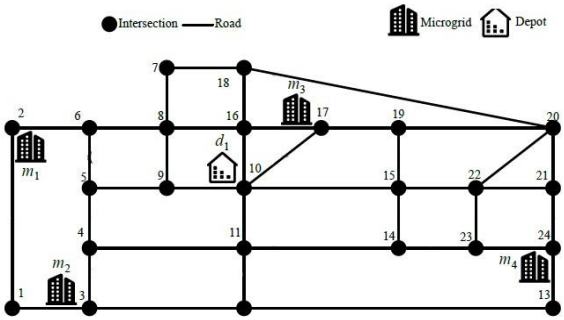

Fig. 5 The Sioux Falls TN along with MGs of DS.

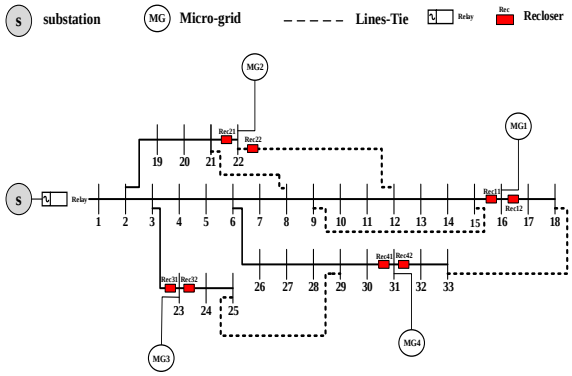

Fig. 6 The modified IEEE 33-bus distribution test system with the protection system.

Table 1 Parameters of the MESS fleet.

MESS	1	2	3
$\bar{P}_{ch}$ (kW)	200	200	200
$\bar{P}_{dch}$ *(kW)*	300	300	300
η_{ch}	0.95	0.95	0.95
$\underline{SOC}/\overline{SOC}$ *(pu)*	0.1/0.9	0.1/0.9	0.1/0.9
SOC_0 *(p.u)*	0.5	0.5	0.5
C_{bat} *($/kWh)*	0.01	0.01	0.01
C_{tran} *($/h)*	0.01	0.01	0.01
V_{avg} *(km/h)*	7	7	10

Table 2 Generation resources data of MGs.

MG	1	2	3	4
P_{max}*(kW)*	200	250	100	500
Q_{max}*(kVAr)*	150	180	75	350
E_{min}*(kWh)*	3500	3000	3500	3000
E_{max}*(kWh)*	34500	30700	34500	30700
C_{gen} *($/kWh)*	0.93	0.85	1.15	1.05
Min PF	0.8	0.8	0.8	0.8

The TN was studied by graph theory to determine the best traffic route from the depot to the desired MG, and optimization models were solved using the MOSEK solver in MATLAB software. The settings and coordination of protection devices in DS should be responsive to all cases of reconfiguration and islanding of one or more MGs. Therefore, by calculating the maximum current of each branch as well as short-circuit currents at a time interval for all islanding modes of MGs, a suitable TMS has been determined to coordinate the primary relay with other secondary protection equipment. In this study, normal overcurrent relays and the re-closers are coordinated. This study considers 24 nodes, 3 MESS devices with an initial charge of 50%, and a depot (the initial location of the MESSs). The number of MGs and depots can be changed. As shown in Fig. 5, the MGs are located at nodes #2, #3, #17, and 24, and the depot is in node #10. The edge is a route from the source node to the sink node. According to the number of connections between nodes, 38 routes from each node to other nodes are defined. When the MESS stops at a node for charging or discharging, the source and sink nodes are the same, and 24 edges are considered. Considering 38 return routes or 38 new edges, there are 100 edges numbered from 1 to 100 in the TN. The basic information of the MESSs and MGs are listed in Tables 1 and 2. Also, the demand active and reactive data, load outage cost, and MGs locations are given in Table 3.

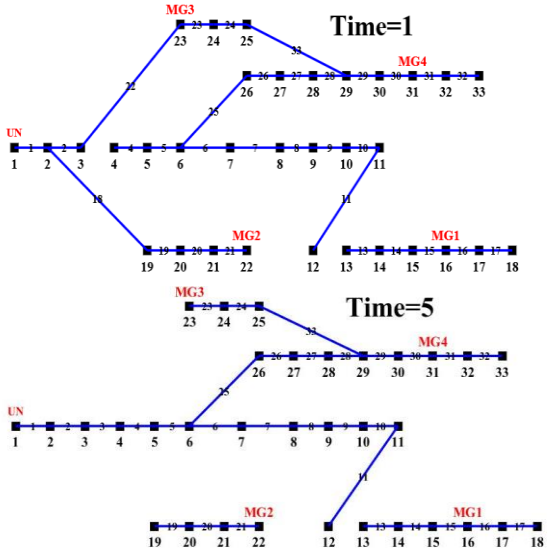

Fig. 7 Reconfiguration of DS at t= 1 and 5 with the islanding of MG#1 and MG#2.

4.1 Prioritization, loads weight, and reconfiguration

After an incident, some MGs may be islanded. To restore the curtailed critical loads, the proposed

model is run based on second objective function. For example, if both MG #1 and MG #2 were islanded, the model would compare the production cost of these MGs and their load shedding costs, taking into account the cost of operation and transportation of MESSs. Accordingly, MG#1 would have a higher priority than MG#2 to send MESS.

Table 3 Demand data and load outage costs at different buses.

Bus	Active power	Reactive power	Load outage cost ($/kWh)	Location of MGs
1	0	0	2	0
2	100	60	10	0
3	90	40	2	0
4	120	80	2	0
5	60	30	2	0
6	60	20	2	0
7	200	100	2	0
8	200	100	10	0
9	60	20	2	0
10	60	20	2	0
11	45	30	2	0
12	60	35	2	0
13	60	35	2	0
14	120	80	2	0
15	60	10	2	0
16	90	20	2	MG1
17	60	20	10	0
18	90	40	2	0
19	90	40	2	0
20	90	40	2	0
21	90	40	2	0
22	90	40	2	MG2
23	90	50	10	MG3
24	420	200	2	0
25	420	200	10	0
26	60	25	2	0
27	60	25	2	0
28	60	20	10	0
29	120	70	2	0
30	200	600	100	0
31	150	70	100	MG4
32	210	100	100	0
33	60	40	100	0

It is worth noting that the configuration of the DS can be updated based on the latest information on the damaged branches of DS and their subsequent repair. As it is shown in Fig. 7, two reconfigurations have been carried out at t=1 and t=5 while MG#1and MG#2 were islanded at t=1. Similarly, MESS fleets are scheduled or re-routed during the restoration period according to most recent status of road damages and routes reparation.

4.2 MG# 1 islanding

For better illustration of MESS fleets scheduling, the islanding of MG#1 after an event in studied in this scenario. Before the event, the DS was in normal condition, and the MESSs were in the depot with 50% initial SOC. When the event occurred at t=1, MG#1 became islanded, and the DS was reconfigured as depicted in Fig. 8. Then, the MESSs start moving from the depot after receiving the initial information. Figures 9 to 11 show the charging and discharging of MESS, blocking and repairing traffic routes, and returning to the depot at different time intervals. As depicted in Fig. 9, MESSs at t=2 start moving toward MG#3 to increase their SOC while the route between nodes 5 and 6 was blocked (arc#8). At the end of interval 6th, MESSs were fully charged, and they moved to MG#1 for load restoration (Fig. 10). They arrived at MG#1 at the end of t=10 and they were there until t=19. When the MESSs discharged to their minimum SOC at the end of t= 19, they were moved to the depot (Fig. 11).

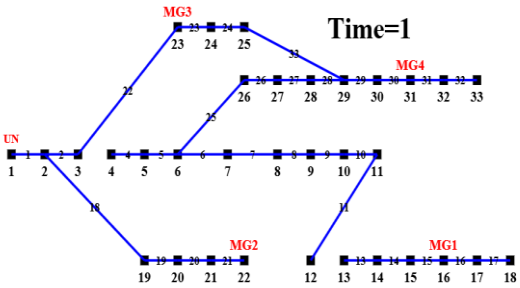

Fig. 8 MG#1 islanding and DS reconfiguration at t=1.

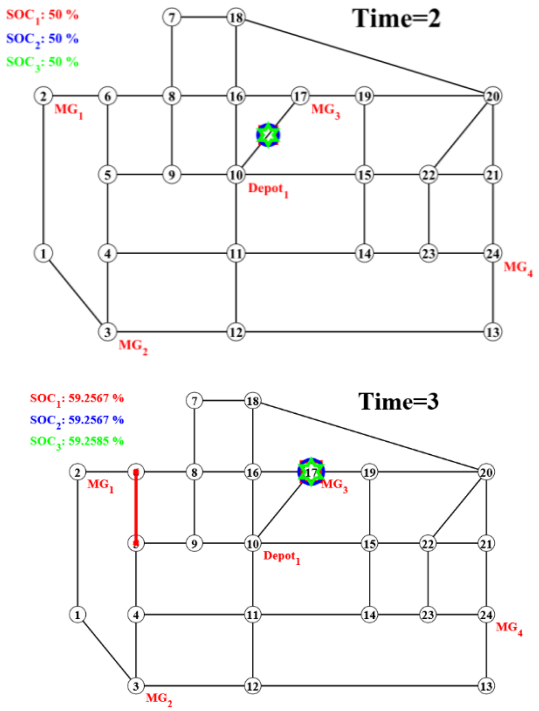

Fig. 9 MESSs moved to increase their SOCs while the arc#8 (route 5 to 6) is blocked

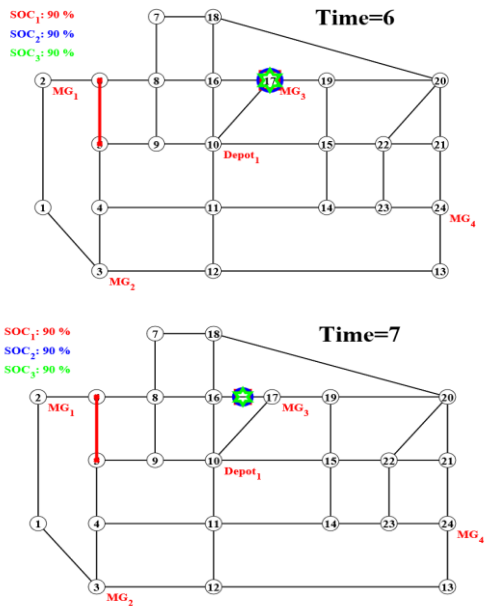

Fig. 10 Increasing the charge of MESSs in MG #3 to the allowable limit and their movement toward the target bus.

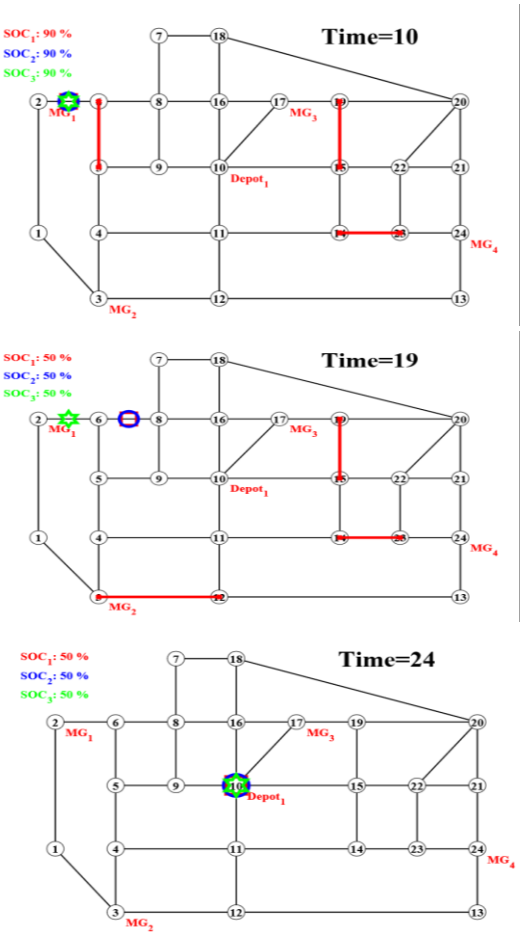

Fig. 11 Discharging in MG#1, and then returning to the depot.

As mentioned, MESSs are connected to MG#1 from time interval 11 to 18. During this time, some curtailed loads are restored by MESS. With the departure of MESSs at t=19, the energy required by MG#1 is not fully supplied. This indicates that the presence of MESSs improves the enhanced grid resilience, and it is well demonstrated by the DRI index given in Table 4.

Table 4 The effect of the presence of MESS in improving the resilience index.

Time	$\mathrm{DRI} = \mathrm{DRI}_{\mathrm{load}} - \mathrm{GRI}_{\mathrm{DG}}$	
	Without presence MESS ($GRI_{DG} = 0$)	With presence of MESS ($GRI_{DG} \neq 0$)
11	86	0
12	99	2
13	109	6
14	84	2
15	49	0
16	6	0
17	75	0
18	110	5

After occurrence of an event, the current of the branches will change. So, all branch currents should be calculated. Table 5 compares the maximum branch currents and the maximum short circuits for 10 branches. These current are calculated for normal network mode (without fault) and islanding of MG#1.

Table 5 Comparison of passing current and short circuit in normal and islanding of MG#1.

Branch	Source bus	Sink bus	Maximum current in normal mode	Maximum current in island mode (# 1)	Maximum short circuit current in normal mode	Maximum short circuit current in island mode (# 1)
1	1	2	137/17	122/67	28477	28477
2	2	3	118/67	110/77	9101	9101
3	3	4	3/344	34/47	6026/9	6026/9
4	4	5	6.95	31/24	879/42	4457/2
5	5	6	10/17	29/74	926/36	2711/7
6	6	7	19/95	27/21	995/72	2281/4
7	7	8	9/98	17/85	773/68	1375/8
8	8	9	0	11/115	0	1110/8
9	9	10	3/09	8/25	557/07	993/79
10	10	11	0	5/59	0	910/94

As can be seen, the initial protection settings may not work properly in islanding conditions, and may lead to protection malfunction. Accordingly, protection coordination is investigated to further explore the effectiveness of the proposed model. First, the protection coordination is performed for the normal condition (Case 1). Then, three other cases are considered for examining the protection coordination of different models after post event.

Case 1: Normal network condition (Pre-event)

The maximum branch currents and their associated maximum short-circuit currents for normal network situation, where none of the MG are islanded, are shown in Figs. 12 and 13. The pick-up current was calculated with an overload factor of 1.5 for each branch.

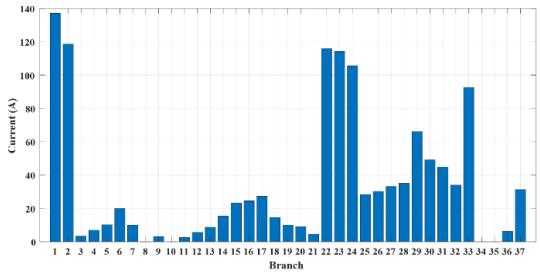

Fig. 12 Maximum branch current under normal network conditions.

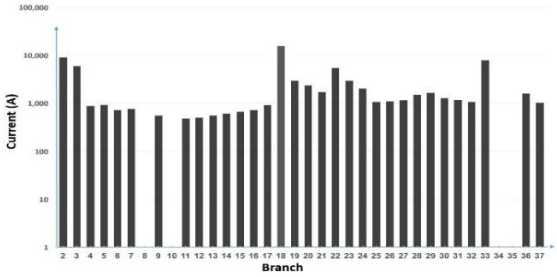

Fig. 13 Maximum short circuit current of each branch under normal situation.

As detailed in Table 6, it can be observed that the relay operates earlier than the reclosers for TMS = 0.05 in the default mode. Because recloser #32 has the longest operating time than other reclosers, the new TMS was considered with a minimum interval of 0.3 from the recloser operating time. This creates coordination between the primary relay and the secondary relays. These settings are performed in conditions where the network operates normally and all MGs are connected.

Case 2: Fixed TMS for Pre- and Post- events

In this case, the initial settings and TMS of the relay in normal network (pre-event) condition are considered for post event, too. The TMS for relay and reclosers are set to 0.3 and 0.05, respectively. Fifteen different network states are considered to investigate the coordination performance. According to Fig. 14, in many states, the operating time difference between the reclosers and the relay violates the 0.3, this will be considering as lack of protection coordination. For example, when MG#1, MG#3, and MG#4 are disconnected from the network, the operating time difference between recloser #21 and the upstream relay reaches below 0.3.

Table 6 Proper TMS under normal network condition.

Normal network condition (no event)

$$t_{op} = \frac{TMS \times \beta}{\left(\frac{I_F}{I_P}\right)^{\alpha} - 1}, \alpha = 0.02, \beta = 0.14$$

Branches	*From*	*To*	*NO-Rec*	*NO-CB*	Ip = Ib *1.5	If	t_{op} (TMS=0.05)	T rel-Trec	T rel=Trec+0.3	t_{op} (TMS=0.31)	Trel new-Trec
1	1	2		1	205.8	28447	0.07		0.419	0.4195	
15	15	16	12		35.0	666	0.12	-0.05	0.415	0	0.30
16	16	17	11		36.8	727	0.11	-0.05	0.414	0	0.31
21	21	22	21		6.8	17186	0.04	0.03	0.341	0	0.38
22	3	23	31		173.9	5447	0.10	-0.03	0.398	0	0.32
23	23	24	32		171.5	2955	0.12	-0.05	0.419	0	0.30
30	30	31	41		73.7	1278	0.12	-0.05	0.419	0	0.30
31	31	32	42		67.3	1182	0.12	-0.05	0.419	0	0.30

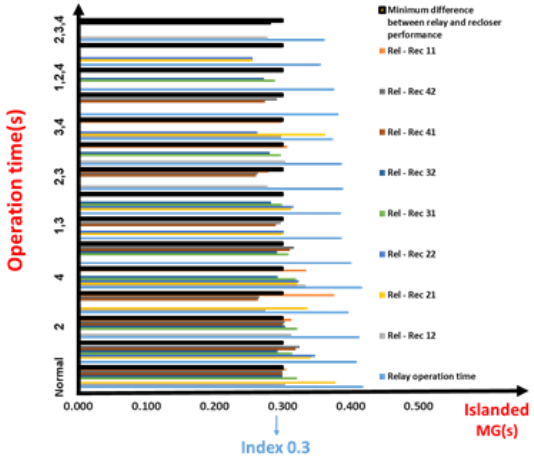

Fig. 14 Operation time difference between the relay and reclosers with TMS setting under normal state.

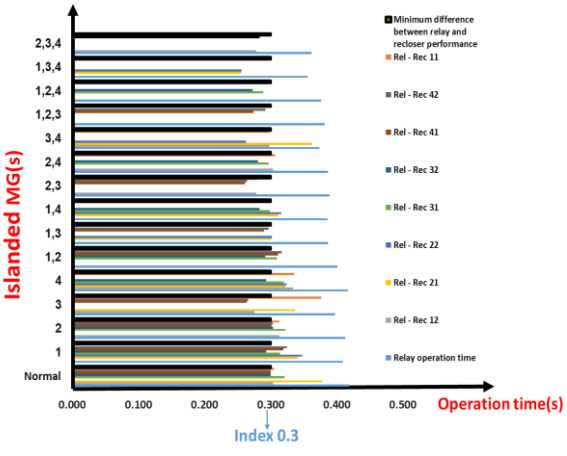

Fig 15 Operating time differences between the relay and reclosers with separate TMS adjustment for each network state

Case 3: Adaptive TMS for Pre- and Post- events

As mentioned in Section 3, two different strategies are considered for this case. In first

strategy, calculation of TMS and adjustment of the relay for post-events are done for each network state. Therefore, an appropriate TMS is obtained, and the relay is set for each reconfiguration and islanding of the MG(s). This way, the appropriate coordination is achieved. As shown in Fig. 15, the coordination between the relay and re-closers is established under all network states. However, this is not possible for traditional DS to send the settings of protection elements under new configurations. Accordingly, the second strategy considers the highest TMS obtained for the final setting of the relay in all network states. According to Fig. 16, the highest TMS is obtained when MG#1, MG#3, and MG#4 are islanded. This TMS is selected for final settings. As it is shown in Fig. 17, this strategy guarantees the coordination of protection system for all 15 network states.

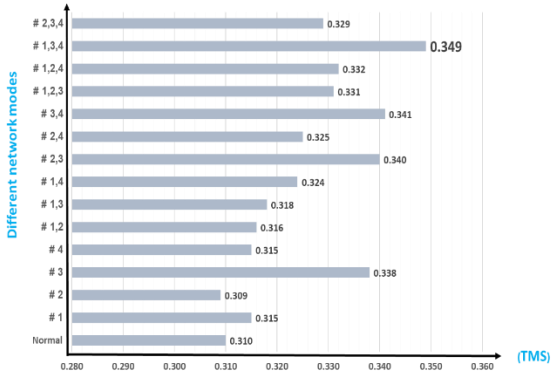

Fig. 16 Comparison of the obtained TMSs and determination of the highest TMS.

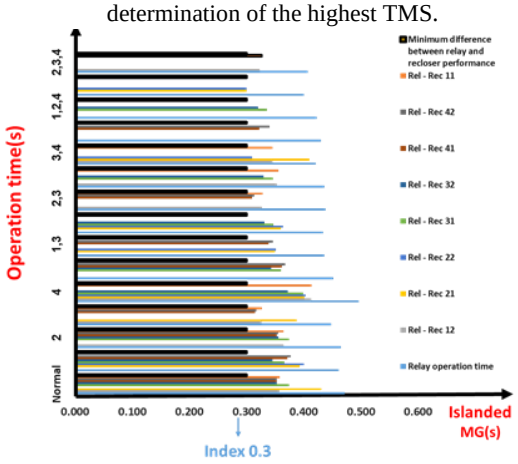

Fig. 17 Operating time difference between the relay and reclosers, considering the final TMS for all network states.

5 Conclusions

This paper proposes a loads restoration strategy to resilience enhancement via minimizing the total system cost while considering MESS fleets, MG formation and protection coordination in DS. The proposed strategy takes into account damage and repair to both the roads in TN and the branches in DS. A rolling optimization framework is adopted to consider subsequent damage and repair during the restoration process. There is the ability to schedule and to make decisions based on the latest data in the optimization process. A comparison of model outputs showed that MESSs, as soon as an event occurs, move through the optimal routes to reach the target MG(s) after receiving instantaneous information about the DS and TN. The results show that the proposed model leading to the restoration of critical loads and improved resilience. It should be noted that the interdependence between the TN and DS have significant impacts on the loads' restoration process. The results indicated that MESSs provide the possibility of more restoration of critical loads via charging from MG(s) or DS resources on the route of movement and discharging into other MG(s). Case studies also confirm that the proposed model successfully provide protection coordination during the load restoration process.

Funding

No funding was received for this work.

CRediT Authorship Contribution Statement

H. Salarvand: Original Draft Preparation, Software and Simulation, Idea & Conceptualization. **M. Doostizadeh:** Revise & Editing, Methodology, Supervision. **F. Namdari:** Analysis, Verification, Supervision

Declaration of Competing Interest

The authors confirm that they have given due consideration to the protection of intellectual property associated with this work and that there are no impediments to publication, including the timing of publication, with respect to intellectual property.

References

[1] C. Chen, J. Wang, and D. Ton, "Modernizing distribution system restoration to achieve grid resiliency against extreme weather events: an integrated solution," *Proceedings of the IEEE*, vol. 105, no. 7, pp. 1267-1288, 2017.

[2] P. Dehghanian, S. Aslan, P. Dehghanian, "Maintaining electric system safety through an enhanced network resilience," *IEEE Transactions on Industry Applications*, vol. 54, no. 5, pp. 4927-4937, 2018.

[3] M. Panteli, and P. Mancarella, "The grid: stronger, bigger, smarter: presenting a conceptual framework of power system resilience," *IEEE power and Energy Magazine*, vol. 13, no. 3, pp. 58-66, 2015.

[4] W. Yuan, J. Wang, F. Qiu, Ch. Chen, Ch. Kang, and B. Zeng, "Robust optimization-based resilient distribution network planning against natural disasters," *IEEE Transactions on Smart Grid*, vol. 7, no. 6, pp. 2817-2826, 2016.

[5] G. Huang, J. Wang, C. Chen, C. Guo, and B. zhu, "System resilience enhancement: Smart grid and beyond," *Frontiers of Engineering Management*, vol. 4, no. 3, pp. 271-282, 2017.

[6] Y. Wang, C. Chen, J. Wang, and R. Baldick, "Research on resilience of power systems under natural disasters a review," *IEEE Transactions on power systems*, vol. 31, no. 2, pp. 1604-1613, 2016.

[7] Y. Xu, C.-C. Liu, K. Schneider, F. Tuffner, and D. Ton, "Microgrids for service restoration to critical load in a resilient distribution system," *IEEE Trans. Smart Grid*, vol. 9, no. 1, pp. 426-437, 2018.

[8] G. Huang, J. Wang, C. Chen, J. Qi, and C. Guo, "Integration of preventive and emergency responses for power grid resilience enhancement," *IEEE Trans. Power System*, vol. 32, no. 3, pp. 4451-4463, 2017.

[9] A. Arab, A. Khodaei, S. K. Khator, K. Ding, V. A. Emesih, and Z. Han, "Stochastic prehurricane restoration planning for electric power systems infrastructure," *IEEE Trans. Smart Grid*, vol. 6, no. 2, pp. 1046-1054, 2015.

[10] C. Lirong, W. Kuo, H. T. Loh, and M. Xie, "Optimal allocation of minimal & perfect repairs under resource constraints," *IEEE Trans. Reliability*, vol. 53, no. 2, pp. 193-199, 2004.

[11] Y. Lin and Z. Bie, "Tri-level optimal hardening plan for a resilient distribution system considering reconfiguration and DG islanding," *Applied Energy*, vol. 210, pp. 1266-1279, 2018.

[12] J. Kim and Y. Dvorkin, "Enhancing distribution system resilience with mobile energy storage and microgrids," *IEEE Transactions on Smart Grid*, vol. 10, no. 5, pp. 4996-5006, 2019.

[13] S. Lei, C. Chen, H. Zhou and Y. Hou, "Routing and scheduling of mobile power sources for distribution system resilience enhancement," *IEEE Transactions on Smart Grid*, vol. 10, no. 5, pp. 5650-5662, 2019.

[14] H. Hassan Abdeltawab, Y. Abdel-Rady and I. Mohamed, "Mobile energy storage scheduling and operation in active distribution systems," *IEEE Transactions on Industrial Electronics*, vol. 64, no. 9, pp. 6828-6840, 2017.

[15] Y. Sun, Z. Li, W. Tian and M. Shahidehpour, "A lagrangian decomposition approach to energy storage transportation scheduling in power systems," *IEEE Transactions on power systems*, vol. 31, no. 6, pp. 4348-4356, 2016.

[16] S. Lei, J. Wang, Ch. Chen and Y. Hou, "Mobile emergency generator pre-positioning and real-time allocation for resilient response to natural disasters," *IEEE Transactions on Smart Grid*, vol. 9, no. 3, pp. 2030-2041, 2016.

[17] S. Yan, J. C. Chu, and Y. L. Shih, "Optimal scheduling for highway emergency repairs under large-scale supply-demand perturbations," *IEEE Transactions on Intelligent Transportation Systems*, vol. 15, no. 6, pp. 2378-2393, 2014.

[18] X. Liu, T. Zhao, S. Yao, C. B. Soh, and P. Wang, "Distributed operation management of battery swapping-charging systems," *IEEE Transactions on Smart Grid*, vol. 10, no. 5, pp. 5320-5333, 2018.

[19] M. Panteli, Dimitris N. Trakas, Pierluigi Mancarella, Nikos D. Hatziargyriou, "Power systems resilience assessment: hardening and smart operational enhancement strategies," *Proceedings of the IEEE*, vol. 105, no. 7 pp. 1202-1213, 2017.

[20] K. S. A. Sedzro, A. J. Lamadrid, and L. F. Zuluaga, "Allocation of resources using a microgrid formation approach for resilient electric grids," *IEEE Transactions on Power Systems*, vol. 33, no. 3, pp. 2633-2643, 2018.

[21] S. Lei, C. Chen, Y. Li and Y. Hou, "Resilient disaster recovery logistics of distribution systems: co-optimize service restoration with repair crew and mobile power source dispatch," *IEEE Transactions on Smart Grid*, vol. 10, no. 6, pp. 6187-6202, 2019.

[22] Z. Bie, Y. Lin, G. Li, and F. Li, "Battling the extreme: a study on the power system resilience," *Proceedings of the IEEE*, vol. 105, no. 7, pp. 1253-1266, 2017.

[23] Y. Wang, C. Chen, J. Wang, and R. Baldick, "Research on resilience of power systems under natural disasters a review," *IEEE Transactions on power systems*, vol. 31, no. 2, pp. 1604-1613, 2016.

[24] G. B. Gharehpetian, M. Shahidehpour and B. Zaker, *Smart Grids and microgrids*. Amirkabir University of Technology (Tehran Polytechnic), 2019.

[25] E. Khoshbakht, F. Namdari and M. Doostizadeh, "Effects of protection settings on optimal performance of reconfigurable smart distribution systems," *IET Renewable Power Generation*, vol. 15, no. 8, pp. 1678-1692, 2021.

[26] Z. Wang, J. Wang, B. Chen, M. M. Begovic, and Y. He, "MPC based Voltage/Var optimization for distribution circuits with distributed generators and exponential load models," *IEEE Trans. Smart Grid*, vol. 5, no. 5, pp. 2412-2420, 2014.

[27] L. Wu, M. Shahidehpour, and T. Li, "Stochastic security-constrained unit commitment," *IEEE Trans. Power System*, vol. 22, no. 2, pp. 800-811, 2007.
[28] T. H. Cormen, *Introduction to algorithms*. MIT press, 2009.
[29] Sh. Yao, P. Wang, X. Liu, H. Zhang and T. Zhao, "Rolling optimization of mobile energy storage fleets for resilient service restoration," *IEEE Transactions on smart grid*, vol. 11, pp. 1030-1043, 2020.
[30] T. Ding, Y. Lin, G. Li, and Z. Bie, "A new model for resilient distribution systems by microgrids formation," *IEEE Power and Energy Society General Meeting (PESGM)*, vol. 32, no. 5, pp. 4145-4147, 2017.
[31] Y. Wang, Y. Xu, J. He, C.-C. Liu, K. P. Schneider, M. Hong, and D. T. Ton, "Coordinating multiple sources for service restoration to enhance resilience of distribution systems," *IEEE Transactions on Smart Grid*, vol. 10, no. 5, pp. 5781-5793, 2019.
[32] M. Bakhshipour, F. Namdari and S. Samadinasab, "Optimal coordination of overcurrent relays with constraining communication links using DE–GA algorithm," *Electrical Engineering*, vol. 103, no. 5 pp. 2243-2257, 2021.
[33] M. E. Baran and F. F. Wu, "Network reconfiguration in distribution systems for loss reduction and load balancing," *IEEE Transactions on Power Delivery*, vol. 4, no. 2, pp. 1401-1407, 1989.
[34] L. J. LeBlanc, E. K. Morlok, and W. P. Pierskalla, "An efficient approach to solving the road network equilibrium traffic assignment problem," *Transportation Research*, vol. 9, no. 5, pp. 309-318, 1975.

Hamid Salarvand received the BSc and MSc degrees in Electrical Power Engineering from Islamic Azad University Borujerd, and Lorestan University in 2010 and 2021, respectively. His fields of interest are Active Distribution Networks, Resiliency, Power System Protection, and Power System Reconfiguration.

Meysam Doostizadeh received the MSc and Ph.D. degrees in Electrical Engineering from the University of Tehran, Tehran, Iran, in 2012 and 2016, respectively. He is currently an Assistant Professor with the Faculty of Engineering, Lorestan University, Khorramabad, Iran. His research interests include electricity markets, smart grid technologies, and integration of renewable energy into power systems.

Farhad Namdari received the BSc in Electrical Power Engineering from Iran University of Science and Technology (IUST) in 1995 and the MSc in Electrical Power Engineering from Tarbiat Modarres University (TMU), Iran in 1998, andthe Ph.D. in Electrical Power Engineering from IUST in 2006. During 1998-2011 he has worked as a Senior Consultant in several Cement Companies in Iran. In 2003, for 11 months, he worked as Honorary Research Associate with Queen's University Belfast, UK. From 2009 he joined Lorestan University, where he is now working as a Professor. Dr. Namdari has published more than 90 technical papers invaluable journals and conferences. His fields of interest are Power System Protection, Power System Transients, Smart Grids, and Artificial Intelligent (AI) Applications in Power Systems, Power System Optimization, and Wide Area Monitoring, Protection, and Control of Power Systems.